Modelling Neck Postural Stabilization Using Optimal Control Techniques for Dynamic Driving

Chrysovalanto Messiou(✉), Georgios Papaioannou, and Riender Happee

Technische Universiteit Delft, Mekelweg 5, 2628 CD Delft, The Netherlands
c.messiou@tudelft.nl

Abstract. The goal of this paper is to contribute to the accurate prediction of human body motion by proposing a novel head-neck model for dynamic driving scenarios with complex vehicle motions. While automated vehicles are considered a potential solution to several transportation issues, there are still significant challenges that need to be addressed, including fundamental questions regarding motion comfort and postural stability. Existing standards fail to accurately describe motion comfort, and current head-neck models have limitations, such as their inability to accurately capture human head responses to dynamic perturbations and lack of adaptability to different perturbations, amplitudes, and individual characteristics. To address these challenges, the authors propose a 3D double inverted pendulum model (DIPM) with a total of 6 degrees of freedom (DoF) as an approximation of head-neck system. The proposed model uses Model Predictive Control (MPC) to derive optimal control inputs for head-neck stabilization. The study validates the proposed model against experimental data of anterior-posterior seat translation and rotation from the literature. The results indicate that the model fitted the experimental data with a variance accounted for 82.80% in translation and 73.15% in rotation (pitch). The proposed model paves the path for the accurate assessment of occupants' postural stability in automated vehicles.

Keywords: Head-neck · postural stabilization · body modeling · dynamic driving · automated vehicles

1 Introduction

Automated vehicles (AVs) have been considered as a potential solution to several issues related to transportation. Meanwhile, AVs should be able to provide increased motion comfort, i.e., reduced motion sickness (MS) and ride discomfort, for AVs occupants to freely engage in non-driving related tasks (NDRT) during their commute. Albeit motion comfort being a pivotal factor for AVs public acceptance, there are still significant challenges that need to be addressed, while fundamental questions regarding MS and postural stability in AVs are still unanswered. Existing standards, like ISO-2631-1 (1997), fail to accurately describe motion comfort, using standardized metrics based on motion frequency. They neglect the effects of vision, postural stability and complex

S. Scataglini et al. (Eds.): DHM 2023, LNNS 744, pp. 177–185, 2023.
https://doi.org/10.1007/978-3-031-37848-5_20

vehicle motions that include coupled translation and rotation. The sensory conflict theory [1–3], the most prominent theory about motion sickness, relates it to mismatches between perceived and expected motion and between sensory modalities (e.g., vestibular, visual, and somatosensory). However, visual, and vestibular sensory systems are head-referenced, and the accurate prediction of the seat to head motion is required. At the same time, head rotations are proven to be strongly related with MS incidence [4], while they are also controlled by vestibular/visual and muscle feedback [5, 6]. Hence, the head-neck system is a critical component of not only controlling human body motion but also for motion comfort.

Numerous neuromuscular neck models have been introduced in literature, including 1-pivot models [7], comprehensive multi-segment models [8], and partial finite element models [9–11]. Nevertheless, there are several limitations with current head-neck models, such as their inability to accurately capture human head responses to dynamic perturbations. Models developed for crash simulation [10] have demonstrated reasonable accuracy in the first 200 ms, but have been observed to become unstable after this period. Several recent models include effective postural stabilization controllers and can simulate human motion in general conditions including prolonged driving. Active head models actuated with PID controllers and including motion perception [5, 6] showed better data fitting for eyes closed compared to eyes open. However, the computational complexity of these models is quite high reporting a computation time of approximately 130 times real-time [6]. At the same time, head neck models lack the ability to adapt to different perturbations, amplitudes, passenger conditions, and individual characteristics while they have increased computational complexity. Thus, the need has risen for more efficient and adaptive models that can better predict human head responses leading to a more accurate motion comfort assessment.

To that end, we develop a robust head-neck model using optimal control techniques to adopt in dynamic driving with complex vehicle motions. More specifically, this paper proposes a DIPM realized in 3D space with a total of 6 DoF as an approximation of the head-neck system. We implement MPC, to derive effective control inputs for head-neck stabilization. The proposed model is validated for anterior-posterior seat translation and rotation using experimental data [12]. The study investigates whether the double inverted pendulum model can effectively capture actual head-neck responses.

2 Methods

2.1 DIPM Setup

To simulate human head-neck dynamics in response to perturbations, the DIPM (Fig. 1), was developed in Simulink's Simscape Multibody environment. The head was approximated as a rigid body with a spheroid solid surface and the neck as two rigid bodies with cylindrical solid rods. Two gimbal joints were included to enable three-dimensional rotation in three directions per joint (y-roll, x-pitch, and z-yaw). The first is located between the base and the first link, the latter between the first and second links. The DIPM was placed on a planar cart-like base, and anterior-posterior perturbations were

applied to simulate dynamic driving scenarios. These perturbations describe the experimentally recorded motion of the trunk. The weight configuration of the DIPM was designed according to anthropometric measures of a 50*th* percentile male [13].

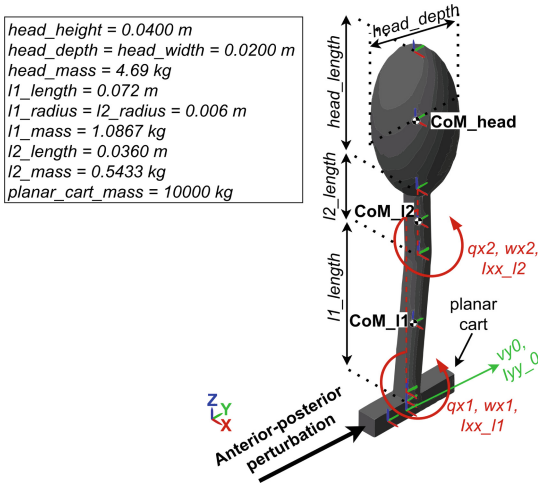

Fig. 1. DIPM free body diagram with dimensions, masses and center of masses (CoM).

2.2 MPC Setup

MPC is an optimal control algorithm seeking to minimize a cost function for a constrained dynamical system, and being able to handle complex and nonlinear systems. To that end, MPC is employed in the DIPM to enable the simulation of the actual head-neck dynamics and overcome the DIPM's highly nonlinear and unstable behavior under perturbations in dynamic driving conditions. The predictive capabilities of MPC allow for the prediction of the head-neck system's future behavior and the optimization of the control action over a finite time horizon while considering system constraints. The communication between the MPC and the DIPM is illustrated in Fig. 2. The MPC was designed using the ACADO optimization tool [14]. To formulate the optimization problem ("MPC block" in Fig. 2), a simplified version of the DIPM was used as the "Prediction Model" in the MPC block. More specifically, the ordinary differential equations (ODEs) of the DIPM were derived using the TMT multibody method in 3D space [15], describing the DIPM kinematics incorporating external forces as linear perturbations at the base and corresponding joint input actuation torques. Finally, the ACADO optimizer was configured by defining the differential states (16), which consist of six states for angular and one linear displacement with their corresponding derivatives (i.e., velocities) of the 6*DoF* DIP and planar cart; six control variables corresponding to the input torques per actuated DoF per joint; three perturbation inputs per x, y, and z-direction. The control time step was set to 0.005 s and the prediction horizon was 25 samples, resulting in a prediction time of 0.125 s. Regarding the "Cost function", two Least Squares Term

(LSQ) minimization functions were implemented; one for the stage cost function, used to capture cost during the control horizon, and one for the terminal cost function. The functions follow the standard definition in ACADO [14], and are as follows:

$$\left\{\begin{array}{c} LSQ\ term: minimize \frac{1}{2}\sum_i \|(h(t_i, x(t_i), u(t_i)) - r\|_S^2 \\ LSQ\ end\ term: minimize \frac{1}{2}\sum_{end} \|(h(t_{end}, x(t_{end})) - r\|_S^2 \\ \\ Constraints: \\ \min(\Theta_x)\text{rad} \leq q_{x1,x2} \leq \max(\Theta_x)\text{rad} \\ \min(\dot{\Theta}_x)\text{rad/s} \leq w_{x1,x2} \leq \max(\dot{\Theta}_x)\text{rad/s} \\ -20\ \text{Nm} \leq t_{x1,x2} \leq 20\ \text{Nm} \end{array}\right\} \quad (1)$$

where h is the differential states; u are the control variables; r is the reference; s is the static weighting vector. To restrict the control outputs of the MPC and maintain the states within the logical boundaries established, constraint functions were implemented (Eq. 1). The constraint functions are imposed on the angles ($q_{x1,x2}$) and angular velocities ($w_{x1,x2}$) of the DIP, and on the input torques ($t_{x1,x2}$). The boundary values were defined as inequality functions, where Θ_x and $\dot{\Theta}_x$ are the experimental angles and angular velocities, respectively.

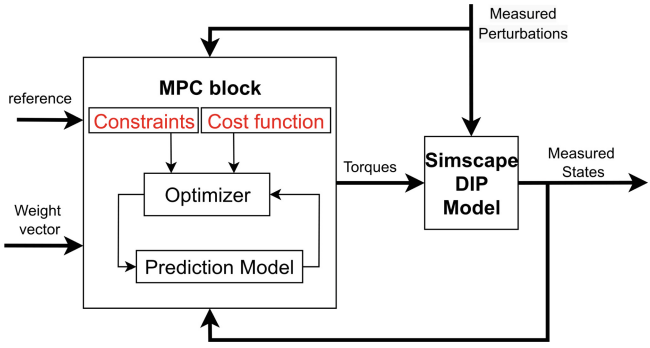

Fig. 2. A block diagram presenting the MPC structure.

2.3 Weight Optimization

The cost weight factors of an MPC controller determine the relative importance assigned to different components of the controller, such as the prediction model and the defined cost functions. Hence, for the simulation of the actual head-neck behavior, the weight vectors used in the LSQ functions (Eq. 1) were optimized to fit the model response to the experimental data. For this, a hybrid algorithm was used combining stochastic global (genetic algorithms – GA) and gradient-based algorithms (MAX4). More specifically, GAs are selected to initiate the optimization since they can handle nonlinear, constrained, and unstable systems, and can find the global optima even when the problem is complex,

and the solution space is large. Then, MAX4 algorithm is used to find the global optimum solution based on GAs solution.

Regarding
the objective functions, the root-mean-square deviation ($RMSE_{\|q(t)\|,\|\Theta(t)\|}$) between the models output (q(t)) and the experimental data (Θ(t)) is used for the GAs. Then, eight objective functions were used in the MAX4 to fine tune the optima, provided by the GAs, towards the global optimum. More specifically, the objectives were the following: $RMSE_{\|q(f)\|,\|\Theta(f)\|}$, $RMSE_{\phi(q(f)),\phi(\Theta(f))}$, $RMSE_{\|w(f)\|,\|\dot{\Theta}(f)\|}$, $RMSE_{\phi(w(f)),\phi(\dot{\Theta}(f))}$, $RMSE_{\|Xmod_{RH}(f)\|,\|X_{RH}(f)\|}$, $RMSE_{\phi(Xmod_{RH}(f)),\phi(X_{RH}(f))}$, $RMSE_{\|\dot{X}mod_{RH}(f)\|,\|\dot{X}_{RH}(f)\|}$ and $RMSE_{\phi(\dot{X}mod_{RH}(f)),\phi(\dot{X}_{RH}(f))}$. Where $Xmod_{RH}$ and $\dot{X}mod_{RH}$ are the model head relative to trunk linear displacement and velocity, while X_{RH} and $\dot{X}_{RH}$ are the experimental head relative to trunk linear displacement and velocity, respectively. The experimental data used as reference for the DIPM were taken from the literature [12], where twelve adult subjects were restrained on a rigid seat with inclined backrest and exposed to pseudorandom multisine perturbations of different bandwidths (0.3–1.2 Hz, 0.3–2.0 Hz, 0.3–4.0 Hz, 0.3–8.0 Hz).

3 Results

This section presents the validation of the DIPM against the experimental data. Firstly, the values of the optimized weights are presented as derived from the hybrid optimization algorithm explained previously. Then, the model response ($Xmod_{RH}$, $\dot{X}mod_{RH}$, q_{x12} and $w_{x1,x2}$) is compared with the experimental data, using time and frequency domain analysis (Figs. 3 and 4). Regarding the frequency domain analysis, the gains, the phase and the coherence are presented. The figures and the optimal weights are discussed in relation to the performance of the DIPM against the experimental data.

3.1 Model Optimized Weights

The weights assigned to the cost function terms in the MPC were optimized as described above to achieve the closest match to the experimental data. The optimized weights signify the relative importance and influence of each parameter on the DIPM's control framework. Moreover, they underscore the necessity of accounting for multiple parameters simultaneously to control the DIPM accurately and simulate the head-neck system's response during anterior-posterior dynamic driving situations with high prediction capabilities.

The angular positions and velocities of the DIPM represent the orientation and movement of the head-neck system in response to the motion of the base cart, which are essential for maintaining postural stability. The large weight assigned to the angle of the second joint ($q_{x2} = 9.5 * 10^4$) in comparison to the first joint ($q_{x1} = 7.4 * 10^3$) indicates that the MPC algorithm prioritizes controlling the motion of the upper link of the DIPM to maintain the stability of the head-neck system. This can be attributed to the fact that the second joint is closest to the head and thus, plays a more significant role in determining the orientation and movement of the head-neck system. The angular position of the second joint determines the orientation of the head relative to the base

cart, while the angular velocity of the second joint determines the rate of change of the head's orientation. Therefore, accurate control of the angle and angular velocity of the second joint is essential for maintaining postural stability during dynamic driving conditions. Additionally, the weights assigned to the angular velocities of both joints ($w_{x1} = 1.0 * 10^4$, $w_{x2} = 4.6 * 10^3$) indicate that the algorithm is designed to respond quickly to changes in the motion of the head-neck system. Finally, the weights assigned to the torques of the two joints ($t_{x1} = 3.0 * 10^2$, $t_{x2} = 9.8 * 10^1$) suggest that the algorithm aims to limit the torque outputs of the joints to ensure safe and feasible control. By limiting the torque outputs of the joints, the MPC algorithm can prevent the DIPM from moving too fast or too forcefully. Similarly, real human subjects typically limit the amount of torque they apply to the head-neck system when exposed to dynamic driving

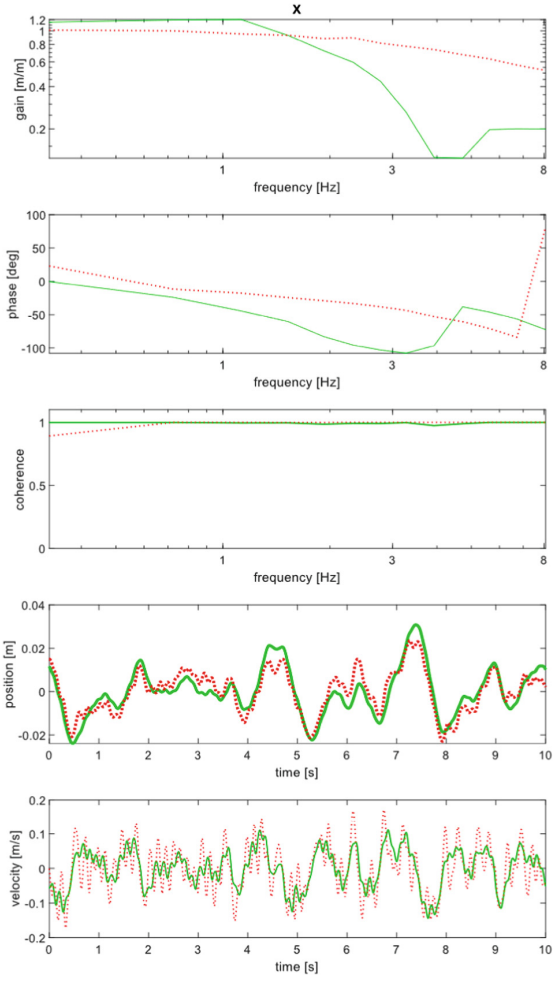

Fig. 3. Comparison of experimental (green continuous line) and model (red dotted line) linear position and velocity of head relative to the trunk in both time and frequency domain

conditions to reduce discomfort and maintain postural stability. The optimized torque weights in the MPC control strategy reflect this behaviour and provide a more accurate simulation of actual human head-neck kinematic behaviour.

3.2 Model Validation

The DIPM was validated against the averaged response from the twelve young subjects. The validation of the DIPM was conducted by comparing $Xmod_{RH}$, $\dot{X}mod_{RH}$ against X_{RH}, $\dot{X}_{RH}$ (Fig. 3) and q_{x12}, $w_{x1,x2}$ against Θ_x, $\dot{\Theta}_x$, respectively (Fig. 4) in both the time and frequency domain. Additionally the coherence is plotted for both the position and

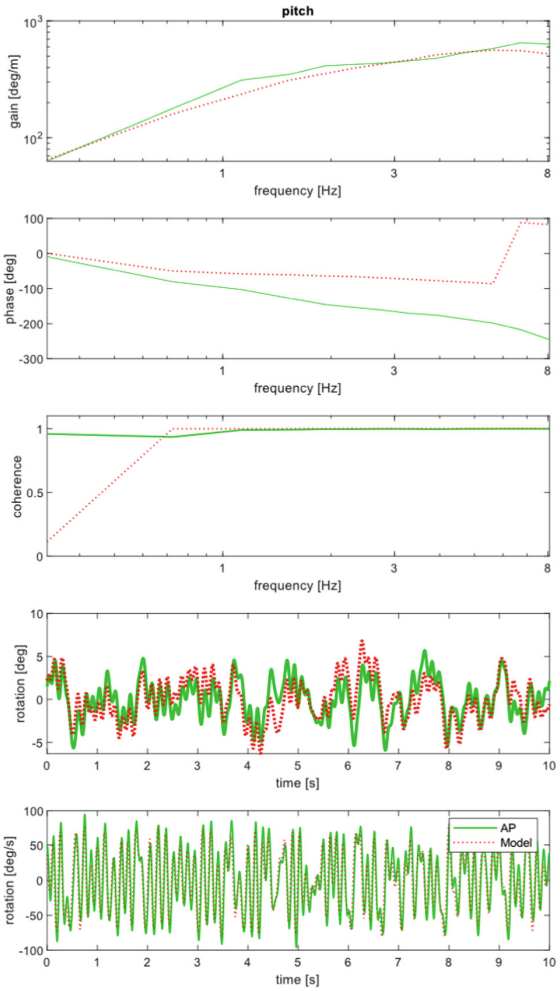

Fig. 4. Comparison of experimental (green continuous line) and model (red dotted line) pitch and angular velocity of head relative to the trunk in both time and frequency domain

pitch signals to show the degree of similarity between the experimental and simulated signals at each frequency.

For the x-position, the model shows a good fit for frequencies below 1.52 Hz, but starts to deviate for higher frequencies, resulting in some high frequency fluctuations in the velocity time domain plot. The phase plot shows that the model response leads the experimental data up until 4.7 Hz and then lags behind it. These differences could be due to the simplified nature of the DIPM, which may not fully capture the complex dynamics of the head-neck system under high-frequency perturbations. However, despite these limitations, the coherence plot shows that the coherence between the model and experimental data is the same for frequencies above 0.7 Hz.

For the pitch, the gain plot in the frequency domain shows a similar trend between the model and experimental data, with the model having more or less the same gain as the experimental data. The phase plot shows that the model response follows a similar trend to the experimental data up until 6.7 Hz, with the model leading the experimental data. Similar to the x-position results, the coherence plot shows that the coherence between the model and experimental data is the same for frequencies above 0.7 Hz, with greater coherence reduction for the simulated data below that frequency. These results suggest that the DIPM captures the main characteristics of the head-neck system for pitch motion, but there are still some discrepancies between the model predictions and experimental data, especially for higher frequencies.

As an additional comparison, the variance accounted for (VAF) was computed for the validation of the DIPM against the experimental data. The VAFs for position and pitch were 82.80% and 73.10%, respectively, resulting in an average VAF of 77.97%. It is important to note that the VAF is an essential performance metric in the validation of biomechanical models and represents the percentage of variability in the experimental data that is accounted for by the model. Therefore, a high VAF indicates a good agreement between the model and the experimental data, which further strengthens the validity and reliability of the DIPM. Furthermore, the simulation time was 2.44 times real time with 0.005 s time step.

In overall, the results suggest that the proposed DIPM is a promising approach for improving the accuracy of predicting human body motion in dynamic driving scenarios. The good fit of the model to experimental data, particularly for the head rotations, which have proven critical for MS accumulation, highlights the potential for this model to be used for motion comfort assessment in dynamic driving scenarios. The limitations observed for higher frequencies in the x-position motion may require further research to determine if other model configurations could improve the prediction capabilities.

4 Conclusion

This paper presents a novel head-neck model for dynamic driving scenarios, which addresses the current limitations of existing models, such as the inability to accurately capture human head responses to dynamic perturbations while being computationally efficient. The validation of the proposed model against experimental data from the literature shows a very good fit, indicating that the model accurately predicts human head-neck behavior. It is important to note that the current DIPM only considers head on trunk control, which is a limitation of the current study. Future works on this model will include

head rotation in space control, which will improve the accuracy of the model for more complex head movements. Additionally, further research is needed to investigate the effect of different types of motion on motion sickness and motion comfort. For example, the current study only considered motion in the sagittal plane, and future studies should examine other types of motion, such as lateral, rotational motion or combinations, such as slalom. Moreover, the current study only focused on data taken from young adult subjects, and future studies should consider including subjects from different age groups and with different health conditions to validate the model's applicability to different populations. Furthermore, the DIPM could be integrated with other models of the human body to develop a more comprehensive understanding of the effects of vibration on the entire body. To sum up, the DIPM developed in this study has promising potential for use in various applications related to motion comfort and motion sickness, and future works will continue to improve and refine the model for more accurate simulations.

References

1. Reason, J., Brand, J.: Motion Sickness. Academic Press, London (1975)
2. Oman, C.M.: Motion sickness: a synthesis and evaluation of the sensory conflict theory. Can. J. Physiol. Pharmacol. **68**(2), 294–303 (1990)
3. Bos, J.E., Bles, W.: Modelling motion sickness and subjective vertical mismatch detailed for vertical motions. Brain Res. Bull. **47**(5), 537–542 (1998)
4. Papaioannou, G., et al.: Assessment of optimal passive suspensions regarding motion sickness mitigation in different road profiles and sitting conditions. In: 2021 IEEE International Intelligent Transportation Systems Conference (ITSC) (2021)
5. Happee, R., et al.: Dynamic head-neck stabilization and modulation with perturbation bandwidth investigated using a multisegment neuromuscular model. J. Biomech. **58**, 203–211 (2017)
6. Happee, R., et al.: Neck postural stabilization, motion comfort, and impact simulation. In: DHM and Posturography, pp. 243–260 (2019)
7. Fard, M., Ishihara, T., Inooka, H.: Dynamics of the head-neck complex in response to the trunk horizontal vibration: modeling and identification. J. Biomech. Eng. **125**, 533–539 (2003)
8. Almeida, J., et al.: Feedback control of the headƁ–ʃneck complex forϭ=nonimpact scenarios using multibody dynamics. Multibody Sys. Dyn. **21**(4), 395–416 (2009)
9. de Bruijn, E., van der Helm, F.C.T., Happee, R.: Analysis of isometric cervical strength with a nonlinear musculoskeletal model with 48 degrees of freedom. Multibody Sys. Dyn. **36**(4), 339–362 (2015)
10. Hedenstierna, S., Halldin, P.: How does a three-dimensional continuum muscle model affect the kinematics and muscle strains of a finite element neck model compared to a discrete muscle model in rear-end, frontal, and lateral impacts. Spine **33**(8), E236–E245 (2008)
11. Meyer, F., et al.: Finite element modelling of the human head-neck: modal analysis and validation in the frequency domain. Int. J. Crashworthiness **9**(5), 535–545 (2004)
12. Forbes, P.A., et al.: Dependency of human neck reflex responses on the bandwidth of pseudorandom anterior-posterior torso perturbations. Exp. Brain Res. **226**, 1–14 (2013)
13. Horst, M.M., Der, V.: Human head neck response in frontal, lateral and rear end impact loading: modelling and validation (2002)
14. Ariens, D., et al.: ACADO for Matlab User's Manual (2010)
15. Schwab, H.V.a.A.L.: Multibody Dynamics, TMT Method, in Advanced Dynamics. 2020: Delft University of Technology (2020)